



# Kent Academic Repository

Raha, A.A., Henderson, J.W., Stott, S.R.W., Vuono, R., Foscarin, S., Friedland, R.P., Zaman, S.H. and Raha-Chowdhury, R. (2017) *Neuroprotective effect of TREM-2 in aging and Alzheimer's disease model*. *Journal of Alzheimer's Disease*, 55 (1). pp. 199-217. ISSN 1387-2877.

## Downloaded from

<https://kar.kent.ac.uk/79837/> The University of Kent's Academic Repository KAR

## The version of record is available from

<https://doi.org/10.3233/JAD-160663>

## This document version

Author's Accepted Manuscript

## DOI for this version

## Licence for this version

UNSPECIFIED

## Additional information

## Versions of research works

### Versions of Record

If this version is the version of record, it is the same as the published version available on the publisher's web site. Cite as the published version.

### Author Accepted Manuscripts

If this document is identified as the Author Accepted Manuscript it is the version after peer review but before type setting, copy editing or publisher branding. Cite as Surname, Initial. (Year) 'Title of article'. To be published in *Title of Journal*, Volume and issue numbers [peer-reviewed accepted version]. Available at: DOI or URL (Accessed: date).

## Enquiries

If you have questions about this document contact [ResearchSupport@kent.ac.uk](mailto:ResearchSupport@kent.ac.uk). Please include the URL of the record in KAR. If you believe that your, or a third party's rights have been compromised through this document please see our [Take Down policy](https://www.kent.ac.uk/guides/kar-the-kent-academic-repository#policies) (available from <https://www.kent.ac.uk/guides/kar-the-kent-academic-repository#policies>).

**Neuroprotective effect of TREM-2 in ageing and Alzheimer's disease model**

Animesh Alexander Raha<sup>a</sup>, James W. Henderson<sup>a</sup>, Simon R.W. Stott<sup>a</sup>, Romina Vuono<sup>a</sup>, Simona Foscarin<sup>a</sup>, Robert P. Friedland<sup>b</sup>, Shahid H. Zaman<sup>c</sup> and Ruma Raha-Chowdhury<sup>a\*</sup>.

<sup>a</sup>John Van Geest Centre for Brain Repair, Department of Clinical Neuroscience,

<sup>b</sup>University of Louisville School of Medicine, Louisville, Kentucky, USA,

<sup>c</sup>Cambridge Intellectual & Developmental Disabilities Research Group, Department of Psychiatry, University of Cambridge, Cambridge, UK,

Running title: **Neuroprotection by TREM2 in Alzheimer's disease**

**\*Corresponding author:**

Ruma Raha-Chowdhury PhD

John Van Geest Centre for Brain Repair

Department of Clinical Neuroscience

University of Cambridge

Cambridge CB2 0PY

Telephone: + 44 1223 331160

Fax: + 44 1223 331176

Email: [rr224@cam.ac.uk](mailto:rr224@cam.ac.uk)

**Abstract:**

Neuroinflammation and activation of innate immunity are early events in neurodegenerative diseases including Alzheimer's disease (AD). Recently, a rare mutation (R47H) in the gene Triggering receptor expressed on myeloid cells 2 (TREM2) has been associated with a substantial increase in the risk of developing late onset Alzheimer's disease. To uncover the molecular mechanisms underlying this association we investigated the RNA and protein expression of TREM2 in APP/PS1 transgenic mouse brain (APP/PS1-tg2576).

Our findings suggest that TREM2 not only plays a critical role in the inflammation, also plays a role in neuronal cell survival and in neurogenesis. We have shown that TREM2 is a soluble protein transported by macrophages through ventricle walls and choroid plexus then enters in the brain parenchyma via radial glial cells. TREM2 protein is essential for neuroplasticity and myelination. Later in life lack of TREM2 protein may accelerate ageing processes and neuronal cell loss and reduce microglial activity, ultimately that leads to neuroinflammation. As inflammation plays a major role in neurodegenerative diseases, a lack of TREM2 could be a missing link between immunomodulation and neuroprotection.

---

Keywords: Alzheimer' disease, choroid plexus macrophages, innate immunity, Neuroinflammation, immunomodulation, myelination, neurogenesis, neuroprotective, neuroplasticity, Soluble TREM2.

## **Introduction**

The immune system has evolved to defend against pathogens and clear up endogenous defective cells (plaques/dying neurons), it is thus conceivable that the immune system may be actively be involved in Alzheimer' disease (AD). Molecules of both the innate and adaptive immune responses are induced in a wide range of neurological disorders, including AD [1, 2], Parkinson's disease (PD) [3-5], Huntington's disease [6], amyotrophic lateral sclerosis (ALS) [7], and multiple sclerosis [8]. There is a highly organized innate immune response during the early stages of inflammation. This inflammatory response is characterized by the expression of various immunological proteins in the circumventricular organs (CVOs), choroid plexus (CPs) and other structures lacking the protection conferred by the blood–brain barrier (BBB) [9, 10]. The response extends progressively to affect microglia and macrophages across the brain parenchyma and may lead to the onset of an adaptive immune response [11, 12].

Alzheimer's diseases (AD) is characterized by the presence of extracellular amyloid deposits comprised of aggregated  $\beta$ -amyloid ( $A\beta$ ) peptides and intracellular neurofibrillary tangles containing hyperphosphorylated, aggregated tau protein [13, 14]. The deposition of  $A\beta$  in brain areas involved in cognitive functions is assumed to initiate a pathological cascade that ultimately results in inflammation, synaptic dysfunction, synaptic loss and neuronal death [15, 16].

Triggering receptor expressed on myeloid cells 2 (TREM2) is a microglia/macrophage receptor that acts as a sensor for a wide array of lipids including apolipoprotein (ApoE) and Phospholipid transfer protein (PLTP) [17-20].

Recent genome-wide association studies have shown that a rare mutation (R47H) of TREM2 gene is associated with a substantial increase in the risk of developing AD [19-22]. The absence of TREM2 expression on microglia impairs their capacity to phagocytose cell membrane debris and increases their production of pro-inflammatory cytokines [23, 24]. Identification of this novel variant in the gene encoding for TREM2 has refocused attention onto inflammation as a major contributing factor in AD [25, 26]. DNAX-activating protein of 12kDa (DAP12, also called TYROBP) is a type I transmembrane adapter proteins which associates with the cytosolic portion of TREM2, forming a molecular complex [17, 27]. It is expressed in neurons, microglia and resident macrophages in the CNS [28] and functions to stimulate phagocytosis and to suppress cytokine production and inflammation [29]. Developmental dysregulation of either TREM2 or DAP12 mutation causes an early onset form of dementia with cystic bone disorder, known as Nasu-Hakola disease [30-32].

Several mouse models that mimic some of the neuropathological and behavioral features of AD have been developed [33-36]. Transgenic mice expressing human APP695 containing the double mutation Lys670-Asn, Met 671 Leu (Swedish mutation) and one PS1 mutation (M146V) in tg2576 (APP/PS1-tg2576) displays age-dependent increases in A $\beta$  plaques, activated microglia, and astrocytes and dystrophic neuritis [10, 16, 35, 37]. The effects of TREM2 in an AD mouse models, particularly those upon A $\beta$  plaque load, have been studied in different transgenic mouse models, generating conflicting results; one group reported that the absence of TREM2 decreased A $\beta$  load [38] whereas another group reported that TREM2 deficiency increased A $\beta$  deposit in another AD (5xFAD) mouse model [39]. Both groups showed the presence of TREM2 in the microglia or in the peripheral macrophages. However, none of these papers have mentioned of the TREM2 protein expression in

the neurons or other glial cells (e.g. in astrocytes or oligodendrocytes).

The aim of our study was to investigate TREM2 protein expression in the APP-PS1 transgenic mouse model of AD to validate both previous and novel findings regarding the location of TREM2 in mouse brain and in vitro analysis using primary neuron and glial culture. Collectively, our data demonstrates that in the young mouse brain TREM2 protein is expressed in pyramidal neurons and dentate gyrus granule cells, indicating a developmental role in neuronal cell survival and neurogenesis. During the early stages of the AD like phenotype in the APP-PS1 mice (between 3-6 months) activated microglia and astrocytes were visible close to the A $\beta$  plaques but TREM2 protein did not co-localised with microglial markers (Iba1 or CD11b) or GFAP positive astrocytes. Furthermore, we show that TREM2 protein levels decline with age that may affect neuronal survival. This may causes the failure of clearance of amyloid deposits by microglia in APP-PS1 mouse brain.

## **Materials and methods**

### **Transgenic mice**

Transgenic mice over expressing the 695-amino acid isoform of human Alzheimer  $\beta$ -amyloid (A $\beta$ ) precursor protein containing a Lys<sup>670</sup>  $\rightarrow$  Asn, Met<sup>671</sup>  $\rightarrow$  Leu mutation (K670N and V717F, Swedish mutation) and one PS1 mutation (M146V), driven by Thy1 promoter on a C57BL/6 genetic background (Tg2576) were purchased from Jackson Laboratory, USA. Neuropathological characterisation of these animals has previously been described in detail [10, 35]. At 3–4 months, these mice start accumulating amyloid deposition and plaques formation, by 9-12 months they resemble a more severe stage of AD pathology [10]. All animals were housed under

standard conditions (12h light-dark cycle, 20°C ambient temperature) with free access to food and water. All procedures were performed under license in accordance to the UK Animals (Scientific Procedures) Act 1986.

Six mice per age group (3, 6, 9 and 10-12 months-old) were used for RT-PCR, immunohistochemistry. Similarly, six mice from each group used for protein quantitation by Western blotting (WB), described subsequently. C57/BL mice were used as control samples (n=6, age-matched to APP-PS1 mice).

### **Tissue preparation**

Mice were terminally anaesthetized with carbon dioxide and culled. Unfixed tissues were dissected from various brain regions from control and APP-PS1 mouse brains and snap frozen in dry ice until analyzed by either RT-PCR or Western blotting as described previously [40]. For histochemical analyses, animals were anesthetized with pento-barbitone and flash-perfused transcardially with 0.9% saline followed with 4% (v/v) paraformaldehyde (PFA) in 0.1 M phosphate buffer (pH 7.4). Brains were sectioned by microtome as described previously [41]. Free-floating sections were prepared (25µm coronal sections in 0.1 M PBS) through the entire olfactory bulb, hippocampus, cortex, mid brain and cerebellum. Sections were then stained by immunohistochemistry as described below.

### **RNA isolation and RT-PCR**

For RNA analysis mouse brain (n = 6) tissues were dissected from frontal cortex (that also contains blood vessels and endothelium) as described above. RNA was extracted from approximately 50 mg of tissue and 1 ml of TRIzol reagent (Invitrogen) following manufacturer's instructions and then purified using an RNeasy Mini kit

(Qiagen). RNA was treated with DNase I, and cDNA synthesised from 2 µg of the treated RNA using a SuperScript III reverse transcriptase kit (Invitrogen) with random hexamer primers. PCR of the newly synthesized cDNA (8 ng) was performed using PCR Supermix (Invitrogen) with the primer pairs for TREM2 (Forward Primer: GCTGCTGATCACAGCCCTG, and Reverse primer: CTTGATTCCTGGAGGTGCTG, product size 464 bp), and DAP12 (Forward Primer: GTGCCTTCTGTTCCCTCCTG and Reverse primer: GGCATAGAGTGGGCTCATCTG, product size 335 bp) using a program of 95°C for 3 min, 30 cycles of 95°C for 30 s, 60°C for 30 s and 72°C for 1 minute. Transcript expression levels were normalised to the expression of GAPDH (Forward Primer: CGGAGTCAACGGATTTGGTCGTAT, Reverse primer: AGCCTTCTCCATGGTGGTGAAGAC, product size 500 bp). PCR products were separated on 1.5 % agarose gels and photographed under UV illumination.

### ***In situ* hybridisation (ISH)**

Brain tissues were prepared for *in situ* hybridization and probed as described previously [40].

### **Synthesis of DIG labelled probes for ISH**

To synthesize digoxigenin (DIG)-labeled RNA probes, the target TREM2 cDNA was amplified by PCR using primers designed on the basis of the mouse TREM2 cDNA sequence used in RT-PCR. The primers used for DIG labeling were

(TREM2-insF: TAATACGACTCACTATAGG GCTGCTGATCACAGCCCTG and TREM2-insR: ATTTAGGTGACACTATAGAGGCATAGAGTGGGCTCATCTG).

The PCR product was amplified using a 5' primer containing a T7 phage promoter sequence and a 3' primer containing an SP6 phage promoter sequence, generating a template for transcription of a sense and an antisense probe, respectively. The PCR products (470 bp) were sequenced and homology checked by BLAST search (NCBI database). *In vitro* transcription reactions were performed using dig-UTP RNA labeling mix (Roche, Mannheim, Germany) and SP6 or T7 RNA polymerase (Roche).

### **ISH with DIG labelled probe**

Brain, liver and other sections were fixed in 4% PFA for 10 min, permeabilized for 10 min in PBS with 0.5% Triton X-100 and acetylated by 10 min incubation in a solution made of 250 ml of water with 3.5 ml of triethanolamine and 625  $\mu$ l of acetic anhydride added drop wise [40]. Pre-hybridization was performed in hybridization buffer made of 50% formamide, 5  $\times$  SSC and 2% blocking reagent (Roche) for 3 hours at 62°C. Hybridization with DIG-labeled probes (100 ng/ml) was performed in the same buffer overnight at 62°C. Stringency washing was performed in 0.2  $\times$  SSC for 1 hour at 62°C. For the detection of DIG-labeled hybrids, the slides were equilibrated in maleic acid buffer (0.1 M maleic acid and 0.15 M NaCl, pH 7.5), incubated for 1 hour at room temperature with 1% blocking reagent made in maleic acid buffer (blocking buffer), and then for 1 hour with alkaline phosphatase-conjugated anti-DIG antibodies (Roche) diluted 1:5000 in blocking buffer. The slides were washed twice for 30 minutes in maleic acid buffer and incubated overnight in colour development buffer [2.4 mg levamisole (Sigma), 45  $\mu$ L 4-nitroblue tetrazolium (Sigma) and 35  $\mu$ l 5-bromo-4-chloro-3-indolyl-phosphate (Sigma) in 10 ml of a buffer made of 0.1 M Trizma base, 0.1 M NaCl and 0.005 M MgCl<sub>2</sub>, pH 9.5]. The reaction was stopped in neutralizing buffer (0.01 M Trizma base and 0.001 M EDTA, pH 8)

and sections mounted in PBS–glycerol and a coverslips applied. Non-specific binding was analysed using sense probes (data not shown).

### **Sources of antibodies**

The following primary antibodies were raised against mouse TREM2 peptides, goat polyclonal (PAB) anti-TREM2 (ab95470) or rabbit polyclonal anti-TREM2 (ab175525) and for human cell line mouse monoclonal (Ab201621). Other antibodies used include anti-TREM2 (HPA010917, Sigma-Aldrich), rabbit PAB synaptophysin, rabbit PAB synapsin (from Abcam, Cambridge, UK). The monoclonal anti- $\alpha\beta$  antibodies (6E10) (Signet laboratory) had been described previously [10] and rabbit anti- $\alpha\beta$  (1-40) and CD11b (Millipore), anti-GFAP (Sigma-Aldrich), Iba1 (WAKO) are described in Table 1. Alexa Fluor 568-labelled donkey anti-mouse, Alexa Fluor 488-labelled donkey anti-rabbit, and Alexa Fluor 568-labelled donkey anti-goat (all from Invitrogen, 1:1000 for IF).

### **SDS-PAGE and western blotting**

Protein lysates were prepared from cortex of mouse brains (n =6), from primary cell culture and neuronal cell line (n=3). 20  $\mu\text{g}$  protein samples were separated on 4-12% Nu-PAGE Bis-tris (Bis (2-hydroxyethyl)-amino-tris (hydroxymethyl)-methane) gradient gels and transferred to 0.2  $\mu\text{m}$  pore size PVDF membranes, using NuPAGE electrophoresis system (Invitrogen). Membranes were incubated with the with TREM2 (rabbit polyclonal anti-TREM2 (ab175525) antibody in blocking buffer for 24 h at 4°C and then washed three times with 0.1 M tris saline buffer containing 1% Tween 20 (TBST) followed by incubation for 1 hour at room temperature with HRP-conjugated secondary antibodies (anti rabbit IgG (1:3000, DAKO) or anti-mouse IgG

(1:3000; DAKO) antibodies). Binding was detected with ECL Plus chemiluminescence reagents.

### **Immunofluorescence (IF)**

Sections were blocked using blocking buffer (0.1 M PBS, 0.1% Triton X100, 10% normal donkey serum) for 1 h at room temperature, then incubated overnight at 4°C with primary antibody diluted in blocking buffer. Alexa Fluor-conjugated secondary antibodies were used for detection and samples counterstained with 4'-diamidino-2-phenylindole (DAPI, Sigma). Sections were then mounted on glass slides with coverslips using FluorSave (Calbiochem).

### **Primary Rat hippocampal cultures**

Cultures of dissociated hippocampal neurons were prepared using previously described methods [42] with some modifications. Hippocampal tissue was collected from Sprague-Dawley (SD) rat embryos (Charles River) at day 18 of development, digested in 0.25% trypsin for 15 min at 37 °C in Hank's buffered saline solution (HBSS) and then gently triturated in Dulbecco's modified Eagle's medium (DMEM) supplemented with 10% fetal calf serum and an additional 0.8% of glucose. This produced a single cell suspension that was plated at a density of  $5 \times 10^4$  cells/cm<sup>2</sup> on glass coverslips coated with 250µg/ml of poly-D-lysine (PDL, Sigma). Cultures were maintained in Neurobasal medium supplemented with 2% B27 and 1% GlutaMAX, and used in experiments after 3 – 4 weeks in culture. Coverslips were fixed with 80% ice-cold methanol and analyzed by IF staining as above and examined by confocal microscopy. All cell culture media and reagents were purchased from Invitrogen.

## **Neuronal cell lines**

Neuronal cell lines (SKNF1 and SH5SY) were plated on PDL coated glass cover slips (as described above) in 24 wells plate with Dulbecco's modified Eagle's medium (DMEM, Gibco), 10% fetal calf serum and 1% penicillin–streptomycin–fungizone (PSF). After 1-3 days *in vitro* cells were fixed with 80% ice-cold methanol and analyzed by IF.

## **Primary rat microglial culture and LPS treatment**

The cortices of new-born SD rats (between P1 to P5) were removed, stripped of the meninges and then chopped up with a razor blade and incubated in 0.1% trypsin (Sigma) in EDTA for 45 min at 37 °C. Following a 5 min incubation in DNase (0.001%, Sigma in HBSS), the supernatant was removed and tissue triturated in 2 ml of triturating solution with a flame-polished Pasteur pipette. After centrifugation for 3 min at 1000 *g*, cells were re-suspended in culture medium [in Dulbecco's modified Eagle's medium (DMEM, Gibco), 10% fetal calf serum, Sera Lab, UK; 1% penicillin–streptomycin–fungizone (PSF), Gibco] and plated in 75 cm<sup>3</sup> poly-l-lysine-coated tissue culture flasks (Nunclon, Life Technologies, Paisley, Scotland) at a density of 2 cortices per flask. To prepare the microglial culture, after the cells became confluent mixed glial cultures were agitated on a rotary shaker at 200 r.p.m for two hours. Floating microglial cells were washed and re grown in a 75 cm<sup>3</sup> flask and some cells were plated on 13-mm-diameter poly- l-lysine-coated coverslips at a density of 10<sup>4</sup> per coverslip. After 1-3 days *in vitro* the culture medium in each well

was changed, and the cells were treated for 4 h with 100nM of LPS and then washed with PBS and fixed as described above.

### **Microscopy**

Bright field images were taken and quantified using Lucia imaging software and a Leica FW 4000 upright microscope equipped with a SPOT digital camera. Fluorescence images were obtained using a Leica DM6000 wide field fluorescence microscope equipped with a Leica FX350 camera and x20 and x40 objectives. Images were taken through several z-sections and de-convolved using Leica software. A Leica TCS SP2 confocal laser-scanning microscope was used with x40 and x63 objectives to acquire high-resolution images.

### **Image and statistics analysis**

All experiments were performed in triplicate. Western blot and immunofluorescence images were quantified using ImageJ software (NIH). For Western blots, the gel analyzer module was used. Selected bands were quantified based on their relative intensities, adjusted for background with fold-change in intensity subjected to statistical analysis as described below. Immunofluorescence was quantified using methods previously described [16]. Values in the figures are expressed as mean  $\pm$  SEM. To determine the statistical significance, values were analyzed by Student's t-test when comparing difference between case (APP-PS1 brain) and controls. A probability value of  $p < 0.05$  was considered to be statistically significant.

## Results:

### **TREM2 in wild-type mouse brain**

As a first step in determining possible roles of TREM2 in the brain, we have investigated the expression of TREM2 and its binding partner DNAX-activating protein of 12kDa (DAP12, also called TYROBP) in wild-type (WT) mouse brain over time. DAP12 is a type I transmembrane adapter proteins which forms a molecular complex with TREM-2 [17, 27]. RT-PCR of TREM2 and DAP12 was performed on tissues from the frontal cortex of 3, 6, 9 and 12 months old WT mice (n = 6 per group). TREM2 levels demonstrated a gradual increase over time in the control mice, peaking at 9 months of age (Figure 1a). DAP12, on the other hand, remained consistent over time (Figure 1b), significantly higher than TREM2 at 3 and 6 months. These measures indicated that both TREM2 and DAP12 are present in the brain.

To investigate the cellular localization of TREM2 mRNA *in situ* hybridization experiments were performed using a TREM2 probe (470bp) amplified by DIG labeling. Despite the presence of RNA based on RT-PCR, very little TREM2 signal was detected in the cortex of WT mice (Figure 1e). Low levels of signal was observed around blood vessels in the brain (Figure 1f), with strong TREM2 transcripts inside the blood vessels, specifically in the mononucleated cells (Figure 1h). Specificity of our probes was demonstrated by labelling TREM2 transcripts in bone osteoclast cells (Figure 1i) and in the stellate macrophages or Kuffer cells of the liver (Figure 1g; [43, 44] and a  $\beta$ -actin probe was used on sections from hippocampus to assess hybridization stringency (Figure 1j). Given the limited localisation of TREM2 mRNA in brain parenchyma, these data suggest that TREM2 is being derived from elsewhere.

WB analysis of frontal cortex from WT mice (at 3, 6, 9 and 12 months, n= 6 per group) complemented the RT-PCR results, indicating that levels of TREM2 protein

increased over the first 6 to 9 months of life (Figure 1k-l). We confirmed the presence of TREM2 protein in the WT mouse brain using immunofluorescent staining. In six-month-old control brains, TREM2 was present in periglomerular neurons, granule cells and white matter tracts of the olfactory bulb (Figure 2a). Similar to the in situ staining, we noted TREM2 immuno staining close to blood vessels, demonstrating co-localized with  $\beta$ -catenin and NG2 positive glia (Figure 2b-c). TREM2 protein was observed in the granular cells of the dentate gyrus in the hippocampus (Figure 2b-c), co-localising with DAPI, whereas no co-localisation with GFAP positive astrocytes and minimal co-localisation with Iba1 positive microglia (Figure 2e-f). TREM2 protein was also present in the cytoplasm and in membrane of the epithelial cells of choroid plexus (Figure 2g-h). Interestingly, TREM2 protein was visible in the pyramidal neurons of layer V-VI of the cortex and it co-localised with A $\beta$ 40 (Figure 2d). This finding suggested that TREM2 protein was present in the neurons, in the oligodendrocytes (in WMT), NG2 positive glia whereas absent in the astrocytes.

### **TREM2 expression in APP mouse brain declined with disease progression**

Given the co-localisation of TREM2 and A $\beta$ 40 in the cortex, we next analyzed the expression of TREM2 in the APP-PS1 mice. RT-PCR of frontal cortex tissue from 3, 6, 9 and 12 months of age, indicated that TREM2 levels were consistently higher in APP-PS1 mice than controls, significantly so at 3 months and 12 months ( $p < 0.001$ ; Figure 1a). Curiously there was no significant difference in DAP12 mRNA levels between the two groups of mice at any time point (Figure 1b). And when we compared TREM2 and DAP12 mRNA in the APP-PS1 brain samples, we noted significantly higher levels of DAP12 at 3 months of age ( $p < 0.0001$ , Figure 1c). GAPDH was used as an internal control (Figure 1d). When we analyzed at protein

levels (via WB), however, we found that TREM2 levels decreased with age and disease progression in the APP-PS1 mice (Figure 1k-l,  $p < 0.001$ ), suggesting post-transcriptional issues for TREM2 in these mice.

To verify further TREM2 protein expression (is it present either in neurons or glial cells?) total cell lysates (within 48 hours of culture) from primary cultures of microglia, mixed glia (includes astrocytes and oligodendrocytes), primary hippocampal culture and a neuronal cell line (SH5SY) were analyzed with mouse monoclonal anti-TREM2 antibody (Ab201621). TREM2 expressed in all proliferative cells, and highest amounts were in hippocampal neurons (Figure 1m). As only two samples were used from each type of cell culture experiments, no statistical analysis was performed. These data confirmed that TREM2 protein was present in early stages of cellular proliferation including in neurons.

### **TREM2 protein in the meningeal macrophages and in surviving neurons in APP-tg mouse brain**

Immunofluorescent staining in the 10 month old APP-PS1 brain presented prominent accumulation of intra-neuronal amyloid throughout the cortex including the frontal and entorhinal cortex, and subiculum and CA1 of the hippocampus (Figure 3a-d). Similar to the WT situation, in ten months old brain TREM2 protein was found to be close to blood vessels (Figure 3e-f). There appeared to be more TREM2 and A $\beta$ 42 co-localisation in cell bodies of the cortex of the APP-PS1 mice, only in surviving neurons (Figure 3a-d). Co-labelling of TREM2 and A $\beta$ 42 was also present in the CA1/2 region of hippocampus (Figure 3a-e), and in close proximity to the plaques in that region, in some cases in the centre of plaques that did not co-localised with GFAP (Figure 3f). Clear expression of TREM2 was seen in the white matter tract of the corpus callosum (Figure 3c), and co-localised with A $\beta$ 42 in the ependymal cells

of choroid plexus (CP; Figure 3g-h). Of interest to us was the presence of TREM2 staining in macrophages on the pial surface of the cortex (indicated by \* in Figure a-b) and in perivascular macrophages in the sub-ventricular zone (SVZ; Figure 3g). This observation - and the blood vessel staining - provided further indications that TREM2 protein is entering the brain via blood vessels and peripheral macrophages.

### **TREM2 protein present in perivascular macrophages in the choroid plexus and the ventricular wall in APP-PS1 mice**

Given the high levels of TREM2 protein expression in blood vessels, SVZ and CP, we turned our attention to the glial cell types in these regions better characterise how TREM2 may be entering the brain. We analyzed sections from 6 and 10 month old APP-PS1 and WT mice. At the 6 months time point, TREM2 protein exhibited limited co-localisation with Iba1+ microglia in the CP of both WT (Figure 4a-c) and APP-PS1 mice (Figure 4d-f). Utilising another microglial marker (CD11b), we also found no co-localisation with microglial cells in both strains of mice (Figure 4g).

Astrocytes are also present in the CP and close to blood vessels, but brain sections stained with TREM2 indicated no co-localisation with GFAP (Figure 4h). To determine entry of TREM2 via blood vessels another section from mid brain stained with TREM2 and IL-10, both protein co-localised in the glial cells (figure 4i). This data suggested that soluble TREM2 protein enters in the brain parenchyma from ventricles, CVO via radial glial cells and was not present in the Iba1 positive activated microglia found in the late stages of disease progression as previously reported by others [28].

## **TREM2 expression in primary neurons, neuronal cell lines and glial precursors**

In order to investigate possible functional roles of TREM2 in the brain, we endeavoured to develop an in vitro assay that could be manipulated. The first step in this process is demonstrating that TREM2 is expressed in vitro. Previous reports have demonstrated limited TREM2 expression in cortical and hippocampal neuronal cultures [26]. In our hands, however, TREM2 was observed in hippocampal neurons (Figure 5a-f), particularly in the soma, at perinuclear location, in axons, dendrites and in the synapses, co-localised with synaptic vesicular protein synaptophysin (Figure 5a-c) and synapsin, indicating soluble TREM2 transportation via axon and dendrites (Figure 5d-f). We confirmed these observations in a second neuronal cell line (SKNF1) noting that both TREM2 and  $\beta$ -III tubulin were seen at perinuclear locations (Figure 5g). To determine TREM2 expression glial precursors (OPC), we analysed mixed glial cultures in very early stages (within 48 hours of plating). TREM2 was present in the perinuclear cytosol in astrocytes and in the growth cones of oligodendrocytes (Figure 5h-i). To confirm TREM2 present was in neuronal precursor (NPC), hippocampal culture (within 48 hours of plating) was stained with BIIT and TREM2, it was present in newly proliferative cells, whereas BIIT was visible in mature neurons (Figure 6a). TREM2 protein was visible in glial precursors (OPC) and co-localised with SOX2 a known transcription factor present in OPC (Figure 6b-c). An astrocyte culture was stained with GFAP and TREM2. A single neuron was stained with TREM2 (shown with an arrow) but no co-localisation of TREM2 in mature astrocytes (Figure 6d). In oligodendrocytes culture TREM2 was visible in the processes and some co-localisation with OPC marker Olig2 in the nucleus (Figure 6

e). This data confirmed that TREM2 was present in all proliferative cells and even in glial precursor cells.

In a third neuronal cell line (SH5SY), we observed TREM2 protein present in the growth cones, suggesting that TREM2 may have important role in cellular differentiation (Figure 6 f-i).

### **TREM2 protein was localized in the Golgi complex and in early endosomes**

As we have noticed TREM2 protein was visible in perinuclear location, dual labeling of TREM2 and Golgi marker (58K-Golgi) was performed in the SKNF1 cell line. TREM2 was observed to co-localize with 58K-Golgi in the trans-Golgi location, suggesting a function in sorting and packaging proteins for secretion (Figure 6j-l). Punctuate TREM2 proteins in the radial glial cells close to the ventricles were observed (Figure 4h), therefore SKNF1 cells were stained with TREM2 and an early endosome marker EEA1. Dual Immunofluorescence labeling shows that both proteins co-localized in the endosomes (Figure 6m-o). EEA1 localizes exclusively to early endosomes and has an important role in endosomal trafficking. Our results suggest that TREM2 protein is transported via EEA1 and is a tethering molecule that provides directionality to vesicular transport from the plasma membrane to the early endosomes.

### **Microglia cultures and responds to LPS treatment**

Finally we assessed TREM2 expression in newly proliferative microglia cultures (Figure 7a-c), and using higher magnification we found TREM2 was visible in the nucleus and perinuclear location but not in the processes and showed limited co-localisation with microglial marker CD11b (Figure 7d-f). These data provided the foundation for investigating roles of TREM2 in vitro.

Inflammation is an important part of neurodegenerative conditions, like Alzheimer's disease [45]. Thus we began our investigation into TREM2 functions by analysing the association of TREM2 in inflammation. Microglia culture was treated with 100 nM of LPS on culture medium for 4 hours. Post-LPS treatment TREM2 expression was increased in some newly proliferative microglia, while mature microglia lost the perinuclear localisation and limited co-localisation was seen with CD11b (Figure 7g-i). We also assessed pro-inflammatory cytokines (IL-1 $\beta$ , TNF $\alpha$  and IL-10) in untreated and in the LPS treated microglia cultures. In untreated microglia, pro-inflammatory cytokines (IL-1 $\beta$ , TNF $\alpha$ ) and IL-10 were expressed in the different subset of organelles within the cells (Figure 7J-k & m). TNF $\alpha$  were expressed in a different population of microglia that had minimal co-localized TREM2 (Figure 7j) or IL-1 $\beta$  (Figure 7k). After LPS treatment both IL-1 $\beta$  and TREM2 proteins was found to be spread throughout the membrane in addition to a change to activated microglial morphology (loss of processes) and limited co-localisation with IL-1 $\beta$ , (Figure 7l). In normal microglia a population of microglia co-localised with CD11b and IL-10 (Figure 7m). After LPS treatment TREM2 co-localized with IL-10 in mixed glial cells (Figure 7n). A significant increase in both TREM2 and IL-1 $\beta$  was detected after LPS treatment (Figure 7o, =P < 0.0001)

## **Discussion**

The association of TREM2 mutations to an increased risk of AD has emphasised the important role played by neuroinflammation in neurodegenerative diseases [19, 20, 46]. Microglia are the only immune cells present in the CNS parenchyma and are the quick responders to environmental changes by playing a critical role in clearing debris and restoring homeostasis in the CNS [47, 48]. With age, the brain undergoes a

homeostatic shift and gradually neuroinflammatory changes develop which compromise neuronal function [29, 49]. In the human brain, TREM2 protein is involved in bone homeostasis, phagocytosis and migration [27, 50, 51].

We have examined TREM2 mRNA levels (by RT-PCR) in APP-PS1 mice and found that TREM2 transcription was age related and increased with age. This could be due to infiltrating macrophages, and such inflammatory changes and have been described in aged APP-PS1 mice which correlate with synaptic function, or it could be due to excessive microglial proliferation due to inflammatory changes in early disease processes [52]. This findings are supported by others published data on TREM2 expression in AD transgenic mice [53]. To identify the cellular location of TREM2 an in-situ hybridisation was performed in C57/BL6 WT mouse brain with DIG labelled TREM2 probe. Surprisingly, very limited cellular expression of TREM2 RNA in the mouse brain was visible only in some cells close to blood vessels in the brain parenchyma and not present in microglia. This could be due to a limited detection level of microglia with DIG labelled probes, however there was a clear signal in the blood/myeloid cells. TREM2 protein expression as measured by Western blotting was also age-dependent in APP-PS1 mice and TREM2 protein levels decreased with age. As we have observed that TREM2 protein is expressed in all precursor cells including in neuronal precursor cells (NPCs) and glial precursor cells (OPCs), it may therefore be involved in cellular proliferation implying that TREM2 deficiency would result in impaired interactions between microglia and plaques as previously reported [54, 55]. TREM2 expression is important in limiting neuronal toxicity during the early stages of A $\beta$  deposition. Only one published paper has thus far reported that TREM2 protein was present in neurons in human brain close to a blood vessels [28]. We have shown that in young WT mice TREM2 protein was highly expressed in the pyramidal

neurons, in the hippocampus and dentate gyrus granule cells, suggesting involvement in cellular plasticity. With age and disease progression TREM2 levels decreased particularly in the frontal and entorhinal cortex, affecting clearing process and plaque burden as seen in APP-PS1 mice and late onset Alzheimer's disease. TREM2 protein was visible in the choroid plexus epithelial cells and in the peripheral macrophages close to the ventricles and subarachnoid space suggested soluble protein carried by macrophages before traversing into the brain. We have shown TREM2 and A $\beta$ 42 to be located in surviving neurons very close to plaques in 3 to 6-month old APP-PS1 mice, whereas with disease progression by 10 months, large swollen dystrophic neurites were associated with A $\beta$  plaques and where no TREM2 was detected. Although Iba-positive activated microglia were clearly visible in the APP-PS1 and WT brain, may be involved in phagocytosis and clearance of plaques. In six-month old WT brain TREM2 was present in the radial glial cells close to the CVO and ventricular walls not co-localising with Iba1, supporting the notion that soluble TREM2 enters in the brain parenchyma via peripheral macrophages as reported previously [38].

In young WT mice TREM2 protein was present in neurogenic niches, therefore we grew primary hippocampal neuron culture to show that TREM2 co-localised with synaptophysin (presynaptic protein) and synapsin (synaptic vesicular protein) in the soma, axon and dendrites. We hypothesised that soluble TREM2 protein could be transported through synaptic vesicles may have a role in synaptogenesis or neurogenesis. TREM2 protein was visible in oligodendrocytes, in the white matter tracts in the cortex, in the olfactory bulb and in striatal bundles indicating that TREM2 protein has a role in myelination so a lack of TREM2 function could be involve in demyelination in demyelinating disorders such as Nasu–Hakola disease,

multiple sclerosis and amyotrophic lateral sclerosis [31, 46]. TREM2 protein was visible in the nucleus and perinuclear area (within the Golgi complex) of all primary cells (OPC and NPCs) and the highest level was seen in growth cone of neurons and oligodendrocytes, further supporting the role of TREM2 in cell proliferation.

In human and mouse neurons and microglia as well as in human cell lines (microglia and glioblastoma), the receptor is mostly localized not at the surface but within the cell: in the perinuclear area in neurons and spread throughout the cytoplasm in microglia and cell lines [56]. The present work has been carried out in neuronal cell line (SKNF1) using immunofluorescence techniques. TREM2 co-localised with the Golgi marker 58K-Golgi, suggesting it may be involved in sorting and packaging of proteins for secretion. It could be involved in the transport of lipids around the cell that when the process was impaired increased the plaques burden in AD. We have seen punctuate TREM2 protein in the radial glial cells close to the ventricles, Therefore we investigated location of TREM2 in endosomes, using a SKNF1 cell line. TREM2 was found to co-localize with an exclusively early endosome marker EEA1. It may present in late endosome too, at present we are investigating role of TREM2 in different endosomal compartment (unpublished findings).

Our results suggest that TREM2 like EEA1 is a tethering molecule that provides directionality to vesicular transport from the plasma membrane to early endosomes. TREM2 is mostly distributed intracellular in two pools: a deposit in the Golgi complex and a population in endo/exocytic vesicles that are continuously translocated to, and recycled from the cell surface as reported previously in a microglia cell line [57]. The identification of TREM2-positive vesicles as organelles competent for regulated exocytosis might open new insights into the study of membrane trafficking and secretion in neuronal cells.

The pro-inflammatory cytokines interleukin-1 $\beta$  (IL-1 $\beta$ ) and tumour necrosis factor- $\alpha$  (TNF- $\alpha$ ) are secreted by activated parenchymal microglial cells and are potent inducers of cell death in animal models of neurodegeneration [58, 59]. Dysfunctional microglia and peripheral macrophages have been shown to contribute to the disease progression in an animal model of ALS [60]. Although innate immune response in the CNS has detrimental effects it was suggested that it has beneficial role too. The release of pro-inflammatory cytokines after acute trauma is followed by a temporal production of neurotrophic factors such as ciliary neurotrophic factor (CNTF) and insulin-like growth factor 1 (IGF1), both involved in the repair of the injured CNS [61]. The presence of TREM2 in the early stages of inflammation and its reduction with age suggests that it might be involve in repair and proliferation [62]. IL-10 is an anti-inflammatory cytokines involved in repair and found to be reduced in AD brain [63].

TREM2 was present in the nucleus in early stages of microglial proliferation. After LPS treatment TREM2 expression increased in newly proliferative microglia and it did not co-localise with TNF- $\alpha$  or IL-1 $\beta$  whereas it co-localised with IL-10 suggesting that TREM2 might have selective anti-inflammatory roles; currently we are investigating possible anti-inflammatory role of TREM2. Furthermore, there might be a physiological function of innate immune mediators, too.

However the functional relevance of innate immune responses in the Alzheimer's disease is not fully understood [64]. It is not clear which components of the innate immunity are leading to neurodegeneration and which parts of the innate immune response are acting neuroprotectively or even neurodegeneratively.

## **Conclusion:**

We have shown that TREM2 is a serum protein transported by macrophages through ventricle walls, CVO and blood vessels entering the brain parenchyma via radial glial cells. TREM2 protein is essential for neuroplasticity, neurotrophism and myelination. Later in life a lack of TREM2 protein may accelerate the ageing process and neuronal cell loss. In all ageing diseases TREM2 levels declined and lack of TREM2 reduced microglial activity leading to neuro-inflammation. As inflammation plays a major role in neurodegenerative diseases, a lack of TREM2 could be the missing link between immunomodulation and neuroprotection.

---

### **Abbreviations**

OB, Olfactory bulb; CP, Choroid plexus; CC, Corpus callosum; CVOs, Circumventricular organs; DAPI, 4'6-diamidino-2-phenylindole; DG, Dentate gyrus; GFAP, Glial fibrillary acidic protein; IHC, Immunohistochemistry; IF, Immunofluorescence; PBS, Phosphate saline buffer; PFA, Paraformaldehyde; PVDF, Polyvinylidene difluoride; SFG, Superior frontal gyrus; SVZ, Sub ventricular zone; TBST, Tris saline buffer with tween; WB, Western blotting; wild type; WT.

### **Competing interest**

The author declared that they have no competing interest.

### **Author's contribution**

AAR, JH performed cell culture, Western blotting, IHC and characterization of APP-PS1 mouse model, IF and confocal microscopy. SS and SF performed in situ, IF and statistical analysis. RV, SS and RPF contributed to the hypothesis development and implications of inflammation in AD brain pathology and edited the manuscript. SZ and RRC contributed to the hypothesis development, performed study design, critically evaluated the results and wrote the manuscript. All authors read and approved the final manuscript.

### **Acknowledgements**

This research was funded by Medical research council (MRC grant number is RNAG/254), National Institute of Health Research (NIHR), The John Van Geest foundation and Cambridgeshire and Peterborough Foundation NHS Trust, Cambridge, UK. We would like to thank Professor Antony Holland for his encouragement and support, Miss Kirah Goldberg, summer student from University of Montreal for participating in histology techniques and to Abcam, Cambridge for providing us TREM2 and other antibodies.

### **References:**

1. Hardy, J., K. Duff, K.G. Hardy, J. Perez-Tur, and M. Hutton, *Genetic dissection of Alzheimer's disease and related dementias: amyloid and its relationship to tau*. Nat Neurosci, 1998. **1**(5): p. 355-8.
2. Selkoe, D.J., D.S. Bell, M.B. Podlisny, D.L. Price, and L.C. Cork, *Conservation of brain amyloid proteins in aged mammals and humans with Alzheimer's disease*. Science, 1987. **235**(4791): p. 873-7.

3. Kim, Y.S. and T.H. Joh, *Microglia, major player in the brain inflammation: their roles in the pathogenesis of Parkinson's disease*. *Exp Mol Med*, 2006. **38**(4): p. 333-47.
4. Whitton, P.S., *Inflammation as a causative factor in the aetiology of Parkinson's disease*. *Br J Pharmacol*, 2007. **150**(8): p. 963-76.
5. Hirsch, E.C., S. Vyas, and S. Hunot, *Neuroinflammation in Parkinson's disease*. *Parkinsonism Relat Disord*, 2012. **18 Suppl 1**: p. S210-2.
6. Moller, T., *Neuroinflammation in Huntington's disease*. *J Neural Transm (Vienna)*, 2010. **117**(8): p. 1001-8.
7. Holmoy, T., *T cells in amyotrophic lateral sclerosis*. *Eur J Neurol*, 2008. **15**(4): p. 360-6.
8. Frohman, E.M., M.K. Racke, and C.S. Raine, *Multiple sclerosis--the plaque and its pathogenesis*. *N Engl J Med*, 2006. **354**(9): p. 942-55.
9. Engelhardt, B., *The blood-central nervous system barriers actively control immune cell entry into the central nervous system*. *Curr Pharm Des*, 2008. **14**(16): p. 1555-65.
10. Raha, A.A., A. Bomford, and R. Raha-Chowdhury, *Hepcidin and Ferroportin Participate in Iron Clearance from Brain Endothelium: Failure of This Process Leads to Iron Accumulation in Alzheimer's Disease*. *American Journal of Hematology*, 2013. **88**(5): p. E156-E156.
11. Schwartz, M. and J. Kipnis, *Protective autoimmunity and neuroprotection in inflammatory and noninflammatory neurodegenerative diseases*. *J Neurol Sci*, 2005. **233**(1-2): p. 163-6.
12. Town, T., V. Nikolic, and J. Tan, *The microglial "activation" continuum: from innate to adaptive responses*. *J Neuroinflammation*, 2005. **2**: p. 24.
13. Hardy, J. and D. Allsop, *Amyloid deposition as the central event in the aetiology of Alzheimer's disease*. *Trends Pharmacol Sci*, 1991. **12**(10): p. 383-8.
14. Spillantini, M.G. and M. Goedert, *Tau pathology and neurodegeneration*. *Lancet Neurol*, 2013. **12**(6): p. 609-22.
15. Walsh, D.M. and D.J. Selkoe, *Oligomers on the brain: the emerging role of soluble protein aggregates in neurodegeneration*. *Protein Pept Lett*, 2004. **11**(3): p. 213-28.
16. Raha, A.A., R.A. Vaishnav, R.P. Friedland, A. Bomford, and R. Raha-Chowdhury, *The systemic iron-regulatory proteins hepcidin and ferroportin are reduced in the brain in Alzheimer's disease*. *Acta Neuropathol Commun*, 2013. **1**: p. 55.
17. Daws, M.R., L.L. Lanier, W.E. Seaman, and J.C. Ryan, *Cloning and characterization of a novel mouse myeloid DAPI2-associated receptor family*. *Eur J Immunol*, 2001. **31**(3): p. 783-91.
18. Cannon, J.P., M. O'Driscoll, and G.W. Litman, *Specific lipid recognition is a general feature of CD300 and TREM molecules*. *Immunogenetics*, 2012. **64**(1): p. 39-47.
19. Guerreiro, R. and J. Hardy, *TREM2 and neurodegenerative disease*. *N Engl J Med*, 2013. **369**(16): p. 1569-70.
20. Jonsson, T. and K. Stefansson, *TREM2 and neurodegenerative disease*. *N Engl J Med*, 2013. **369**(16): p. 1568-9.
21. Tanzi, R.E., *TREM2 and Risk of Alzheimer's Disease--Friend or Foe?* *N Engl J Med*, 2015. **372**(26): p. 2564-5.

22. Slattery, C.F., J.A. Beck, L. Harper, G. Adamson, Z. Abdi, J. Uphill, T. Campbell, R. Druyeh, C.J. Mahoney, J.D. Rohrer, J. Kenny, J. Lowe, K.K. Leung, J. Barnes, S.L. Clegg, M. Blair, J.M. Nicholas, R.J. Guerreiro, J.B. Rowe, C. Ponto, I. Zerr, H. Kretzschmar, P. Gambetti, S.J. Crutch, J.D. Warren, M.N. Rossor, N.C. Fox, J. Collinge, J.M. Schott, and S. Mead, *R47H TREM2 variant increases risk of typical early-onset Alzheimer's disease but not of prion or frontotemporal dementia*. *Alzheimers Dement*, 2014. **10**(6): p. 602-608 e4.
23. Hsieh, C.L., M. Koike, S.C. Spusta, E.C. Niemi, M. Yenari, M.C. Nakamura, and W.E. Seaman, *A role for TREM2 ligands in the phagocytosis of apoptotic neuronal cells by microglia*. *J Neurochem*, 2009. **109**(4): p. 1144-56.
24. Kleinberger, G., Y. Yamanishi, M. Suarez-Calvet, E. Czirr, E. Lohmann, E. Cuyvers, H. Struyfs, N. Pettkus, A. Wenninger-Weinzierl, F. Mazaheri, S. Tahirovic, A. Lleo, D. Alcolea, J. Fortea, M. Willem, S. Lammich, J.L. Molinuevo, R. Sanchez-Valle, A. Antonell, A. Ramirez, M.T. Heneka, K. Sleegers, J. van der Zee, J.J. Martin, S. Engelborghs, A. Demirtas-Tatlidede, H. Zetterberg, C. Van Broeckhoven, H. Gurvit, T. Wyss-Coray, J. Hardy, M. Colonna, and C. Haass, *TREM2 mutations implicated in neurodegeneration impair cell surface transport and phagocytosis*. *Sci Transl Med*, 2014. **6**(243): p. 243ra86.
25. Frank, S., G.J. Burbach, M. Bonin, M. Walter, W. Streit, I. Bechmann, and T. Deller, *TREM2 is upregulated in amyloid plaque-associated microglia in aged APP23 transgenic mice*. *Glia*, 2008. **56**(13): p. 1438-47.
26. Kiialainen, A., K. Hovanes, J. Paloneva, O. Kopra, and L. Peltonen, *Dap12 and Trem2, molecules involved in innate immunity and neurodegeneration, are co-expressed in the CNS*. *Neurobiol Dis*, 2005. **18**(2): p. 314-22.
27. Humphrey, M.B., M.R. Daws, S.C. Spusta, E.C. Niemi, J.A. Torchia, L.L. Lanier, W.E. Seaman, and M.C. Nakamura, *TREM2, a DAP12-associated receptor, regulates osteoclast differentiation and function*. *J Bone Miner Res*, 2006. **21**(2): p. 237-45.
28. Satoh, J., N. Kawana, Y. Yamamoto, T. Ishida, Y. Saito, and K. Arima, *A survey of TREM2 antibodies reveals neuronal but not microglial staining in formalin-fixed paraffin-embedded postmortem Alzheimer's brain tissues*. *Alzheimers Res Ther*, 2013. **5**(4): p. 30.
29. Poliani, P.L., Y. Wang, E. Fontana, M.L. Robinette, Y. Yamanishi, S. Gilfillan, and M. Colonna, *TREM2 sustains microglial expansion during aging and response to demyelination*. *J Clin Invest*, 2015. **125**(5): p. 2161-70.
30. Paloneva, J., T. Manninen, G. Christman, K. Hovanes, J. Mandelin, R. Adolfsson, M. Bianchin, T. Bird, R. Miranda, A. Salmaggi, L. Tranebjaerg, Y. Kontinen, and L. Peltonen, *Mutations in two genes encoding different subunits of a receptor signaling complex result in an identical disease phenotype*. *Am J Hum Genet*, 2002. **71**(3): p. 656-62.
31. Thrash, J.C., B.E. Torbett, and M.J. Carson, *Developmental regulation of TREM2 and DAP12 expression in the murine CNS: implications for Nasu-Hakola disease*. *Neurochem Res*, 2009. **34**(1): p. 38-45.
32. Xing, J., A.R. Titus, and M.B. Humphrey, *The TREM2-DAP12 signaling pathway in Nasu-Hakola disease: a molecular genetics perspective*. *Res Rep Biochem*, 2015. **5**: p. 89-100.

33. Hsiao, K., P. Chapman, S. Nilsen, C. Eckman, Y. Harigaya, S. Younkin, F. Yang, and G. Cole, *Correlative memory deficits, Aβ elevation, and amyloid plaques in transgenic mice*. *Science*, 1996. **274**(5284): p. 99-102.
34. Ashe, K.H., *Learning and memory in transgenic mice modeling Alzheimer's disease*. *Learn Mem*, 2001. **8**(6): p. 301-8.
35. Kumar-Singh, S., D. Pirici, E. McGowan, S. Serneels, C. Ceuterick, J. Hardy, K. Duff, D. Dickson, and C. Van Broeckhoven, *Dense-core plaques in Tg2576 and PSAPP mouse models of Alzheimer's disease are centered on vessel walls*. *Am J Pathol*, 2005. **167**(2): p. 527-43.
36. Ulrich, J.D., M.B. Finn, Y. Wang, A. Shen, T.E. Mahan, H. Jiang, F.R. Stewart, L. Piccio, M. Colonna, and D.M. Holtzman, *Altered microglial response to Aβ plaques in APPS1-21 mice heterozygous for TREM2*. *Mol Neurodegener*, 2014. **9**: p. 20.
37. Frautschy, S.A., F. Yang, M. Irizarry, B. Hyman, T.C. Saido, K. Hsiao, and G.M. Cole, *Microglial response to amyloid plaques in APPsw transgenic mice*. *Am J Pathol*, 1998. **152**(1): p. 307-17.
38. Jay, T.R., C.M. Miller, P.J. Cheng, L.C. Graham, S. Bemiller, M.L. Broihier, G. Xu, D. Margevicius, J.C. Karlo, G.L. Sousa, A.C. Cotleur, O. Butovsky, L. Bekris, S.M. Staugaitis, J.B. Leverenz, S.W. Pimplikar, G.E. Landreth, G.R. Howell, R.M. Ransohoff, and B.T. Lamb, *TREM2 deficiency eliminates TREM2+ inflammatory macrophages and ameliorates pathology in Alzheimer's disease mouse models*. *J Exp Med*, 2015. **212**(3): p. 287-95.
39. Wang, Y., M. Cella, K. Mallinson, J.D. Ulrich, K.L. Young, M.L. Robinette, S. Gilfillan, G.M. Krishnan, S. Sudhakar, B.H. Zinselmeyer, D.M. Holtzman, J.R. Cirrito, and M. Colonna, *TREM2 lipid sensing sustains the microglial response in an Alzheimer's disease model*. *Cell*, 2015. **160**(6): p. 1061-71.
40. Raha-Chowdhury, R., A.A. Raha, S. Forostyak, J.W. Zhao, S.R.W. Stott, and A. Bomford, *Expression and cellular localization of hepcidin mRNA and protein in normal rat brain*. *Bmc Neuroscience*, 2015. **16**.
41. Raha-Chowdhury, R., S.R. Andrews, and J.R. Gruen, *CAT 53: A protein phosphatase 1 nuclear targeting subunit encoded in the MHC Class I region strongly expressed in regions of the brain involved in memory, learning, and Alzheimer's disease*. *Molecular Brain Research*, 2005. **138**(1): p. 70-83.
42. Marland, J.R., D. Pan, and P.C. Batty, *Rac GTPase-activating protein (Rac GAP) alpha1-Chimaerin undergoes proteasomal degradation and is stabilized by diacylglycerol signaling in neurons*. *J Biol Chem*, 2011. **286**(1): p. 199-207.
43. Goncalves, L.A., L. Rodrigues-Duarte, J. Rodo, L. Vieira de Moraes, I. Marques, and C. Penha-Goncalves, *TREM2 governs Kupffer cell activation and explains belr1 genetic resistance to malaria liver stage infection*. *Proc Natl Acad Sci U S A*, 2013. **110**(48): p. 19531-6.
44. Otero, K., M. Shinohara, H. Zhao, M. Cella, S. Gilfillan, A. Colucci, R. Faccio, F.P. Ross, S.L. Teitelbaum, H. Takayanagi, and M. Colonna, *TREM2 and beta-catenin regulate bone homeostasis by controlling the rate of osteoclastogenesis*. *J Immunol*, 2012. **188**(6): p. 2612-21.
45. Heppner, F.L., R.M. Ransohoff, and B. Becher, *Immune attack: the role of inflammation in Alzheimer disease*. *Nat Rev Neurosci*, 2015. **16**(6): p. 358-72.
46. Lill, C.M., A. Rengmark, L. Pihlstrom, I. Fogh, A. Shatunov, P.M. Sleiman, L.S. Wang, T. Liu, C.F. Lassen, E. Meissner, P. Alexopoulos, A. Calvo, A. Chio, N. Dizdar, F. Faltraco, L. Forsgren, J. Kirchheiner, A. Kurz, J.P. Larsen,

- M. Liebsch, J. Linder, K.E. Morrison, H. Nissbrandt, M. Otto, J. Pahnke, A. Partch, G. Restagno, D. Rujescu, C. Schnack, C.E. Shaw, P.J. Shaw, H. Tumani, O.B. Tysnes, O. Valladares, V. Silani, L.H. van den Berg, W. van Rheenen, J.H. Veldink, U. Lindenberger, E. Steinhagen-Thiessen, S. Consortium, S. Teipel, R. Perneczky, H. Hakonarson, H. Hampel, C.A. von Arnim, J.H. Olsen, V.M. Van Deerlin, A. Al-Chalabi, M. Toft, B. Ritz, and L. Bertram, *The role of TREM2 R47H as a risk factor for Alzheimer's disease, frontotemporal lobar degeneration, amyotrophic lateral sclerosis, and Parkinson's disease*. *Alzheimers Dement*, 2015. **11**(12): p. 1407-16.
47. Koizumi, S., Y. Shigemoto-Mogami, K. Nasu-Tada, Y. Shinozaki, K. Ohsawa, M. Tsuda, B.V. Joshi, K.A. Jacobson, S. Kohsaka, and K. Inoue, *UDP acting at P2Y6 receptors is a mediator of microglial phagocytosis*. *Nature*, 2007. **446**(7139): p. 1091-5.
48. Sierra, A., J.M. Encinas, J.J. Deudero, J.H. Chancey, G. Enikolopov, L.S. Overstreet-Wadiche, S.E. Tsirka, and M. Maletic-Savatic, *Microglia shape adult hippocampal neurogenesis through apoptosis-coupled phagocytosis*. *Cell Stem Cell*, 2010. **7**(4): p. 483-95.
49. Costello, D.A., K. Keenan, R.M. McManus, A. Falvey, and M.A. Lynch, *The age-related neuroinflammatory environment promotes macrophage activation, which negatively impacts synaptic function*. *Neurobiol Aging*, 2016. **43**: p. 140-8.
50. Forabosco, P., A. Ramasamy, D. Trabzuni, R. Walker, C. Smith, J. Bras, A.P. Levine, J. Hardy, J.M. Pocock, R. Guerreiro, M.E. Weale, and M. Ryten, *Insights into TREM2 biology by network analysis of human brain gene expression data*. *Neurobiol Aging*, 2013. **34**(12): p. 2699-714.
51. Lampron, A., P.M. Pimentel-Coelho, and S. Rivest, *Migration of bone marrow-derived cells into the central nervous system in models of neurodegeneration*. *J Comp Neurol*, 2013. **521**(17): p. 3863-76.
52. Gate, D., K. Rezai-Zadeh, D. Jodry, A. Rentsendorj, and T. Town, *Macrophages in Alzheimer's disease: the blood-borne identity*. *J Neural Transm (Vienna)*, 2010. **117**(8): p. 961-70.
53. Matarin, M., D.A. Salih, M. Yasvoina, D.M. Cummings, S. Guelfi, W. Liu, M.A. Nahaboo Solim, T.G. Moens, R.M. Paublete, S.S. Ali, M. Perona, R. Desai, K.J. Smith, J. Latcham, M. Fulleylove, J.C. Richardson, J. Hardy, and F.A. Edwards, *A genome-wide gene-expression analysis and database in transgenic mice during development of amyloid or tau pathology*. *Cell Rep*, 2015. **10**(4): p. 633-44.
54. Wang, Y., T.K. Ulland, J.D. Ulrich, W. Song, J.A. Tzaferis, J.T. Hole, P. Yuan, T.E. Mahan, Y. Shi, S. Gilfillan, M. Cella, J. Grutzendler, R.B. DeMattos, J.R. Cirrito, D.M. Holtzman, and M. Colonna, *TREM2-mediated early microglial response limits diffusion and toxicity of amyloid plaques*. *J Exp Med*, 2016. **213**(5): p. 667-75.
55. Yuan, P., C. Condello, C.D. Keene, Y. Wang, T.D. Bird, S.M. Paul, W. Luo, M. Colonna, D. Baddeley, and J. Grutzendler, *TREM2 Haplodeficiency in Mice and Humans Impairs the Microglia Barrier Function Leading to Decreased Amyloid Compaction and Severe Axonal Dystrophy*. *Neuron*, 2016. **90**(4): p. 724-39.
56. Sessa, G., P. Podini, M. Mariani, A. Meroni, R. Spreafico, F. Sinigaglia, M. Colonna, P. Panina, and J. Meldolesi, *Distribution and signaling of TREM2/DAPI2, the receptor system mutated in human polycystic*

- lipomembraneous osteodysplasia with sclerosing leukoencephalopathy dementia*. Eur J Neurosci, 2004. **20**(10): p. 2617-28.
57. Prada, I., G.N. Ongania, C. Buonsanti, P. Panina-Bordignon, and J. Meldolesi, *Triggering receptor expressed in myeloid cells 2 (TREM2) trafficking in microglial cells: continuous shuttling to and from the plasma membrane regulated by cell stimulation*. Neuroscience, 2006. **140**(4): p. 1139-48.
  58. Pasparakis, M., L. Alexopoulou, V. Episkopou, and G. Kollias, *Immune and inflammatory responses in TNF alpha-deficient mice: a critical requirement for TNF alpha in the formation of primary B cell follicles, follicular dendritic cell networks and germinal centers, and in the maturation of the humoral immune response*. J Exp Med, 1996. **184**(4): p. 1397-411.
  59. Beaulieu, L.M., E. Lin, E. Mick, M. Koupenova, E.O. Weinberg, C.D. Kramer, C.A. Genco, K. Tanriverdi, M.G. Larson, E.J. Benjamin, and J.E. Freedman, *Interleukin 1 receptor 1 and interleukin 1beta regulate megakaryocyte maturation, platelet activation, and transcript profile during inflammation in mice and humans*. Arterioscler Thromb Vasc Biol, 2014. **34**(3): p. 552-64.
  60. Boillee, S., K. Yamanaka, C.S. Lobsiger, N.G. Copeland, N.A. Jenkins, G. Kassiotis, G. Kollias, and D.W. Cleveland, *Onset and progression in inherited ALS determined by motor neurons and microglia*. Science, 2006. **312**(5778): p. 1389-92.
  61. Nguyen, M.D., J.P. Julien, and S. Rivest, *Innate immunity: the missing link in neuroprotection and neurodegeneration?* Nat Rev Neurosci, 2002. **3**(3): p. 216-27.
  62. Kipnis, J. and M. Schwartz, *Controlled autoimmunity in CNS maintenance and repair: naturally occurring CD4+CD25+ regulatory T-Cells at the crossroads of health and disease*. Neuromolecular Med, 2005. **7**(3): p. 197-206.
  63. Guillot-Sestier, M.V., K.R. Doty, D. Gate, J. Rodriguez, Jr., B.P. Leung, K. Rezai-Zadeh, and T. Town, *Il10 deficiency rebalances innate immunity to mitigate Alzheimer-like pathology*. Neuron, 2015. **85**(3): p. 534-48.
  64. Guillot-Sestier, M.V., K.R. Doty, and T. Town, *Innate Immunity Fights Alzheimer's Disease*. Trends Neurosci, 2015. **38**(11): p. 674-81.

### **Figure Legends:**

**Figure 1: TREM2 protein level declined with disease progression in APP-PS1 mice.**

Fig 1 a-d: RNA analysis by RT-PCR confirmed an age-dependent increase in TREM2 in the brains of APP and WT mice (a), only statistically significant at 3 and 12 months

age ( $p < 0.01$ ), DAP12 levels were not significant (b), comparison of TREM2 and DAP12 mRNA was significant (c,  $p < 0.001$ ). GAPDH was analyzed as an internal control (d).

Fig 1 e-j: *In situ* hybridization was performed using a DIG labeled TREM2 antisense probe. Very low signal was detected in the frontal cortex of mouse brain (e), around the blood vessels in striatum (f) and in the liver macrophages (g). Clear expression was seen in the blood vessel, specifically in the mononucleated cells, in the brain parenchyma (h) and in the bone cells (i).  $\beta$ -actin probe was used as a positive control (j). *Scale bar*, 150  $\mu\text{m}$  (e), 100  $\mu\text{m}$  (g) and 25  $\mu\text{m}$  (f, h) 20  $\mu\text{m}$  (I & j).

Fig 1 k-m: Western blot (WB) analysis of the brain homogenate from frontal cortex of APP-PS1 and WT (c57/Bl6) mice demonstrated a single 25 kDa band consistent with TREM2 protein (probed with rabbit polyclonal ab175262) was clearly visible within all controls (lane 1; 3m, 2: 6 m, 3: 9 m and 4: 12 m) and APP-PS1 mice (lane 5: 3m, 6: 6 m, 7: 9 m and 8: 12 m) (k). Densitometric analysis of the blots showed that there were significant differences TREM2 levels between APP and control brains were higher in controls, decreased in APP-PS1 brain with age (k & l,  $p = < 0.001$ ).

WB analysis of primary cell culture lysates, (microglia lane 1, 2, mixed glia, lane 3, 4, hippocampus, lane 5, 6, neuronal cell line SH5SY, lane 7 and 8) showed that TREM2 expressed all newly proliferative cells (m). As there were only two cell lysates used from each group, statistical analysis not performed.  $\beta$ -Actin loading control was used to normalize data.

At least three independent experiments were performed for all analyses. Bonferroni-corrected Student's t tests shown;  $n = 6$  per group). Error bars indicate SEM. \* $p < 0.05$ , \*\* $p < 0.01$ , \*\*\* $p < 0.001$ , one-way ANOVA.

**Figure 2: TREM2 protein expression in control mice brain.**

Double immunofluorescence (IFC) staining was performed in six months old control mouse brains with goat polyclonal anti-TREM2 (ab95470; red) and monoclonal anti-GFAP (green) antibodies and counterstained with DAPI for nuclei (Blue). TREM2 immuno-reactivity was visible in molecular layer of olfactory bulb, in glomerular neurons and white matter tracts of the olfactory bulb did not co-localize with GFAP positive astrocytes (a). TREM2 protein (red) was expressed throughout cortex, in the hippocampus and dentate gyrus and there was some co-localization with  $\beta$ -catenine on blood vessels wall (b). TREM2 was present in the dentate gyrus granule cells and some cells co-localized with NG2 (green) positive glia (c). Under higher magnification TREM2 protein was visible in the layer V pyramidal neurons (d), in individual granule cells co-localizing with DAPI but not with GFAP positive astrocytes (e), whereas there was minimal co-localization with microglial marker Iba1 (f). TREM2 protein was present in the cytoplasm and in the membrane of epithelial cells of choroid plexus (g-h). *Scale bar* panels a: 50 $\mu$ m, b: 150 $\mu$ m, d & g: 30 $\mu$ m and c & e 25 $\mu$ m, f & h: 20 $\mu$ m.

**Figure 3: TREM2 protein in the meningeal macrophages and in surviving neurons in APP-PS1 mouse brain.**

Double-label immunofluorescence (IFC) staining of A $\beta$ -42 (green) and TREM2 (red) and DAPI for nucleus was performed in coronal sections from cortex of 6-10 month old APP-PS1-tg2576 mice. In six-month-old APP-PS1 mice, coronal section from frontal cortex (FCX) was stained with TREM2 (red) and A $\beta$ 42 (6E10) green and DAPI (a-d). Severe pathology was evident with amyloid plaques increased in size and quantity and distributed throughout the cortex, TREM2 was observed around the

plaques and in pyramidal neurons, in meningeal macrophages (\* points to pial vasculature, a b). TREM2 protein was visible in hippocampus (CA1, indicating with an arrow) and in subiculum, in the white matter tract of corpus callosum (c), in surviving neurons close to the plaques (d). In ten-month-old APP mice, TREM2 protein was visible in the blood vessels in close proximity to the plaques, did not co-localize with A $\beta$ 42 positive plaques (e). With disease progression dense plaques were visible in the cortex, TREM2 (red) and GFAP (green) positive activated astrocytes were present close to the plaques but did not co-localize with TREM2 (f). In six months old APP-PS1 mice in the lateral ventricle, TREM2 positive macrophages were visible in the choroid plexus, (arrow indicates TREM2 positive macrophages) co-localized with A $\beta$ 42 (green) in appendemal cells (g).  $\beta$ -catenin and TREM2 were visible in the choroid plexus with moderate co-localization and TREM2 positive cells were present close in the CVO (h). At least three independent experiments were performed for all analyses. *Scale bar* panels a: 50 $\mu$ m, b and c: 100  $\mu$ m, d: 15  $\mu$ m, e & f: 25  $\mu$ m, g & h: 50 $\mu$ m.

**Figure 4: TREM2 protein did not co-localize with Iba1 positive activated microglia in the choroid plexus.**

Immunofluorescence (IFC) staining of TREM2 (red) and Iba1 (green) was performed in six-month-old brain sections from lateral ventricle (LV) with choroid plexus (CP) and counterstained with DAPI (blue). Iba1 positive microglia were visible in the choroid plexus where minimal co-localization with TREM2 positive cells (a-c). TREM2 protein was present in the radial glial cells close to the ventricles and did not co-localize with Iba1 positive activated microglia in APP-PS1 mice (d-f). In higher magnification a cortical plaque was stained with CD11b and faint TREM2

expression was seen in the centre of the plaques (g). In SVZ, punctuate vesicular TREM2 was visible in the wall of ventricle, without any co-localization GFAP (h), whereas in the blood vessels TREM2 and IL-10 co-localized (i). *scale bar* a-f: 50  $\mu\text{m}$ , g: 25 $\mu\text{m}$ , h-l: 30  $\mu\text{m}$ .

**Figure 5: Soluble TREM2 was visible in primary hippocampal neurons.**

Confocal microscope analysis of primary hippocampal culture neurons shows that synaptophysin (green) expressed in the synapses (a) and TREM2 (red) was present membrane bound and perinuclear location (b) and visible axon and dendrites in a merge picture (c). Further co-localized with synapsin (d) and TREM2 (e) indicates soluble TREM2 transport might via axon and dendrites (f). SKNF1 cells line was stained with TREM2 (red) and  $\beta$ -III tubulin (green), TREM2 expression was seen at perinuclear whereas  $\beta$ -III tubulin was visible in the process (g). In mixed glial culture very early stages, (within 48 hours of plating) TREM2 (red) was present in the perinuclear location in the GFAP positive (green) astrocytes (h) and in the growth cones of oligodendrocytes indicating with an arrow (i). *The scale bar* in a-f 20 $\mu\text{m}$ , g-100 $\mu\text{m}$ , h-i, 25 $\mu\text{m}$ .

**Figure 6: TREM2 protein was present in different cellular compartments in primary cells and in neuronal cell line.**

Immunofluorescence (IFC) staining of TREM2 (green) and  $\beta$ IIIT (red) was performed in NPCs (a) and OPCs (b-c). TREM2 was visible in NPCs cluster (a) and in glial precursor (b). TREM2 and SOX2 (red) co-localized in the nucleus of OPCs (c). In a glial culture a limited number of neurons were present and stained with

TREM2 (red, indicated with an arrow), did not co-localized with GFAP (green) positive astrocytes (d). TREM2 staining was visible in oligodendrocytes and co-localised with olig2 in the nucleus (e). Neuronal cell line (SH5SY) and stained with A $\beta$ 40 (green) and TREM2 (red), both proteins were present in the growth cones (indicating with an arrow), suggesting that it may have important role in differentiation (f-i). In neuronal cell line (SKNF1) TREM2 (red) and 58K-Golgi (green) co-localised in the Golgi compartment (j-l) and in early endosome stained with EEA1 (green) (m-o). The scale bar in a & e: 50 $\mu$ m, b-d: 25 $\mu$ m, f-i 20 $\mu$ m, i-o: 30 $\mu$ m.

**Figure 7: Microglia cultures and responds to LPS treatment.**

The newly proliferative microglia (after 24 hours) stained with microglial marker CD11b (green) and TREM2 (red) and counterstained with DAPI for nuclear localization. Both proteins were visible in the microglia (a-c). In higher magnification TREM2 was visible in the nucleus and perinuclear location but not in the processes and co-localized with microglial marker CD11b (d-f). In normal microglia, pro-inflammatory cytokines TNF $\alpha$  (j), IL-1 $\beta$  (k) and IL-10 (m) was expressed in different organelles within the cells. After LPS administration TREM2 expression was increased in some newly proliferative microglia, a lost the perinuclear localization in mature microglia and limited co-localization with CD11b (g-i). After LPS treatment, both IL-1 $\beta$  and TREM2 proteins spread through out the membrane and showed activated microglial morphology (loss of processes) and limited co-localization with TREM2 and IL-1 $\beta$  (l) whereas IL-10 and TREM2 co-localized in mixed cell populations (n). The fluorescence intensity indicated a significant increased of TREM2 and IL-1 $\beta$  after LPS treatment (l, =P < 0.0001). *Scale bar* in a-c, g-i and m-n:

50µm, d-f: 20, j-l: 25µm. Error bars indicate SEM. \*p<0.05, \*\*\*p<0.001, one-way ANOVA.

**Table 1. List of the primary antibodies used in this study**

Antibody	Species	Dilution	Supplier/cat. Number
Anti-β 42 (6E10)	Mouse (monoclonal)	1: 1000 for IHC	Covance Cat Number (SIG 39320)
Anti-Aβ40	Rabbit (polyclonal)	1: 500 for IHC	Thermo Fisher Scientific (44348A)
Anti-TREM2	Rat (monoclonal)	1: 1000 for IHC 1:2000 for WB	Abcam (Ab86491)
Anti-TREM2	Rabbit (polyclonal)	1: 200 for IHC 1:1000 for WB	Abcam (ab175262)
Anti-TREM2	Goat (polyclonal)	1:200 for IHC 1:1000 for WB	Abcam (ab95470)
Anti-TREM2	Rabbit (polyclonal)	1: 200 for IHC 1:1000 for WB	Sigma-Aldrich (HPA010917)
Anti-DAP12	Rabbit (polyclonal)	1:500 for IHC	Abcam (ab93846)
Anti β-catenin	Mouse (monoclonal)	1: 1000 for IHC	BD-Biosciences (610153)
Anti-GFAP	Mouse (monoclonal)	1:1000 for IHC	Sigma (G3893 Clone G-A5)
Anti-GFAP	Rabbit	1:200 for IHC	Abcam (ab48050)

	(polyclonal)		
Anti- $\beta$ III-tubulin	Mouse (monoclonal)	1:1000 for IHC	Millipore (clone 2G10, neuronal   05-559)
Anti $\beta$ -actin	Mouse (monoclonal)	1:10000 for WB	<i>Sigma (clone AC-74, A5316)</i>
Anti-CD11b	Mouse (monoclonal)	1:1000 for WB 1:500 for IHC	Chemicon CBL1512
Anti-Iba1	Rabbit (polyclonal)	1:500 for IHC	Wako (019-19741)
Anti-IL-1 $\beta$	Goat (polyclonal)	1:200 for IHC	R&D system (AB-401-NA)
Anti-TNF $\alpha$	Rabbit (polyclonal)	1:250 for IHC	Abcam (ab34674)
Anti-IL-10	Rabbit (monoclonal)	1: 500 for IHC 1:1000 for WB	Abcam (ab133575)
Anti-SOX2	Mouse (monoclonal)	1:1000 for IHC	Abcam (Ab79351)
Anti-Olig2	Rabbit (monoclonal)	1:1000 for IHC	Abcam (ab109186)
Anti-EEA1	Rabbit (polyclonal)	1: 500 for IHC	Abcam (ab2900)
Anti-58K-Golgi	Mouse (monoclonal)	1: 500 for IHC	Abcam (ab27043)
Anti-Synapsin	Rabbit (polyclonal)	1: 1000 for IHC	Abcam (ab8)

Anti-Synaptophysin	Rabbit (polyclonal)	1: 500 for IHC	Abcam (ab32594)
--------------------	---------------------	----------------	-----------------

IHC, immunohistochemistry; WB, Western blot.

Figure 1:

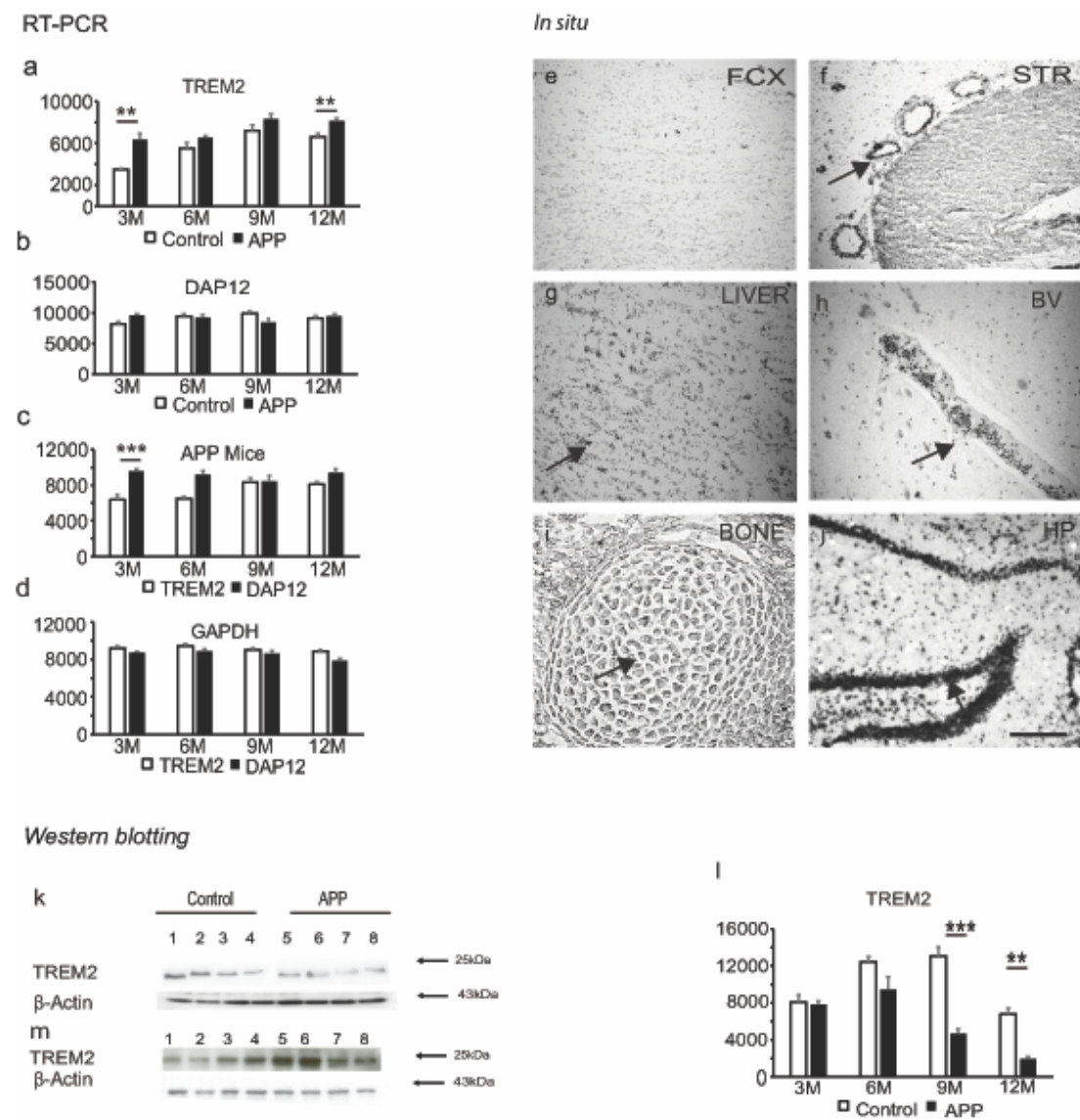


Figure 2:

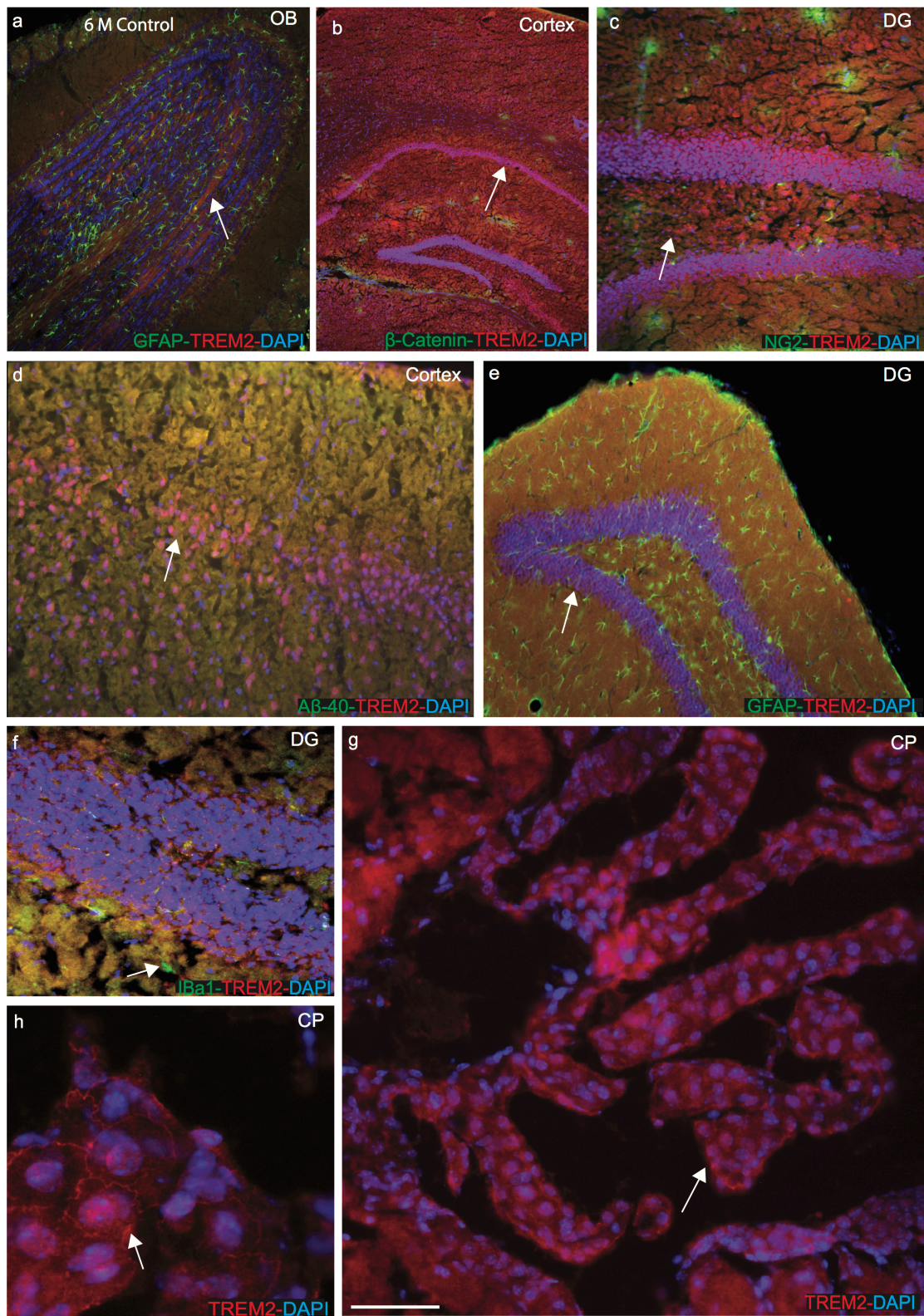


Figure 3:

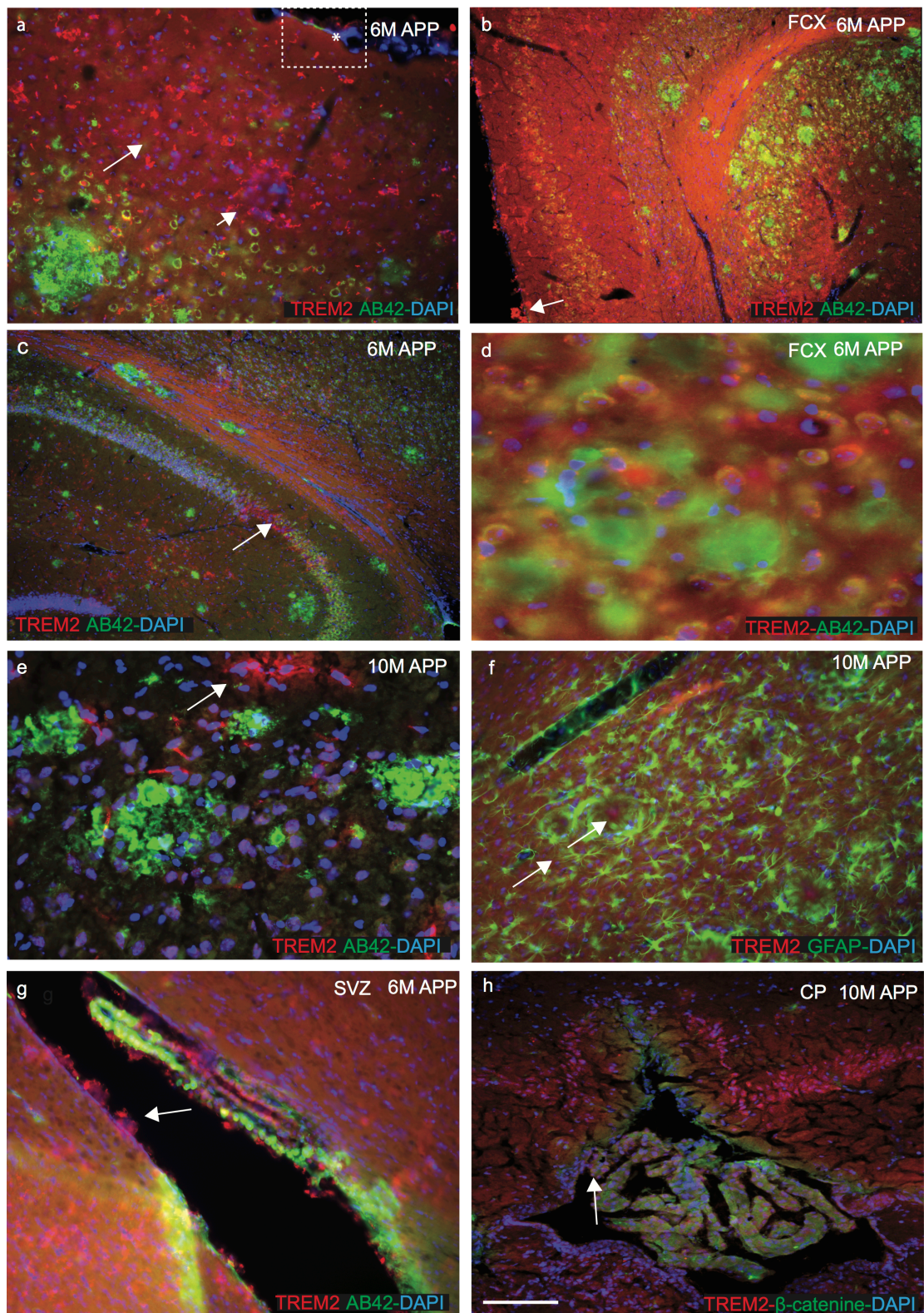


Figure 4

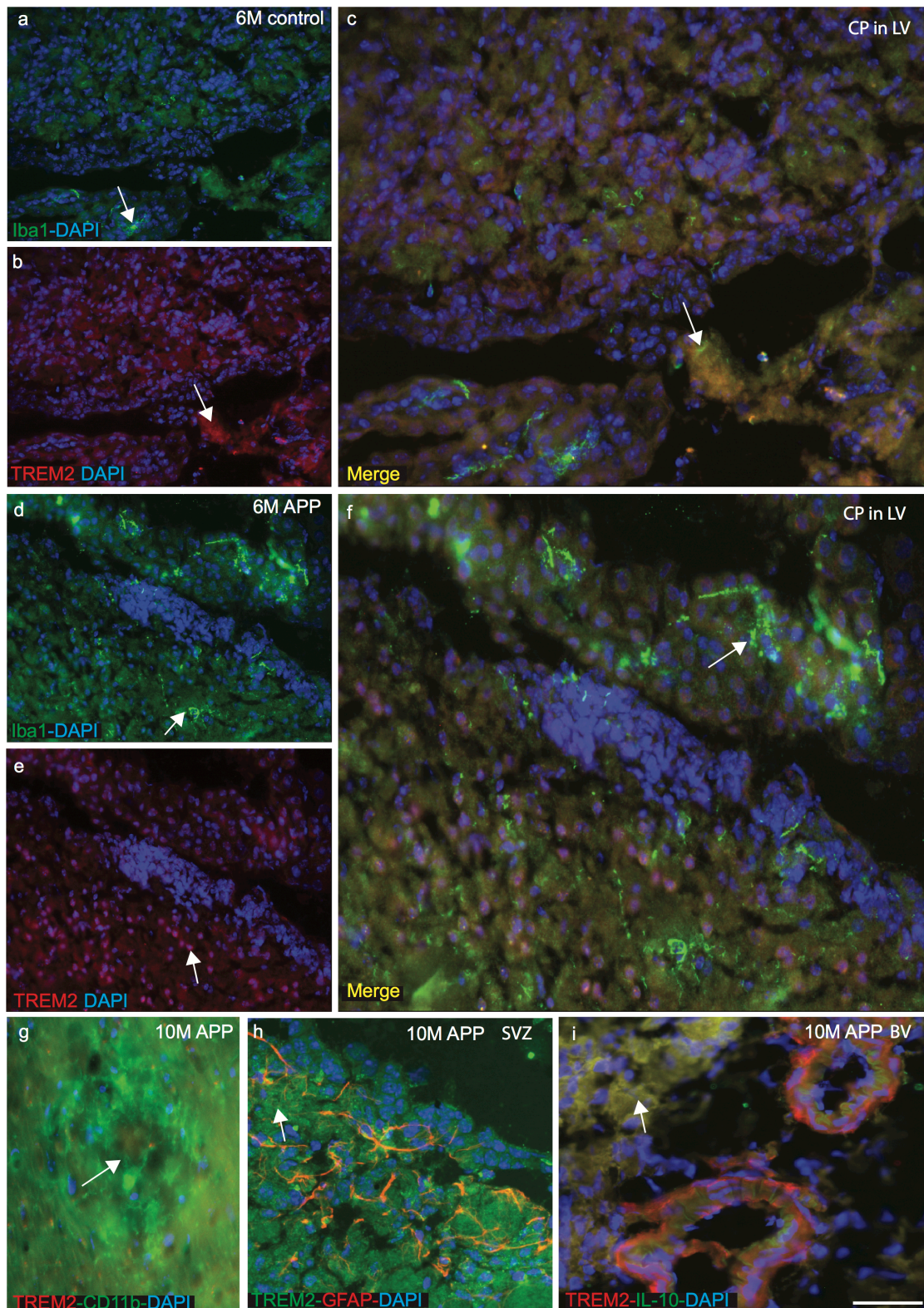


Figure 5:

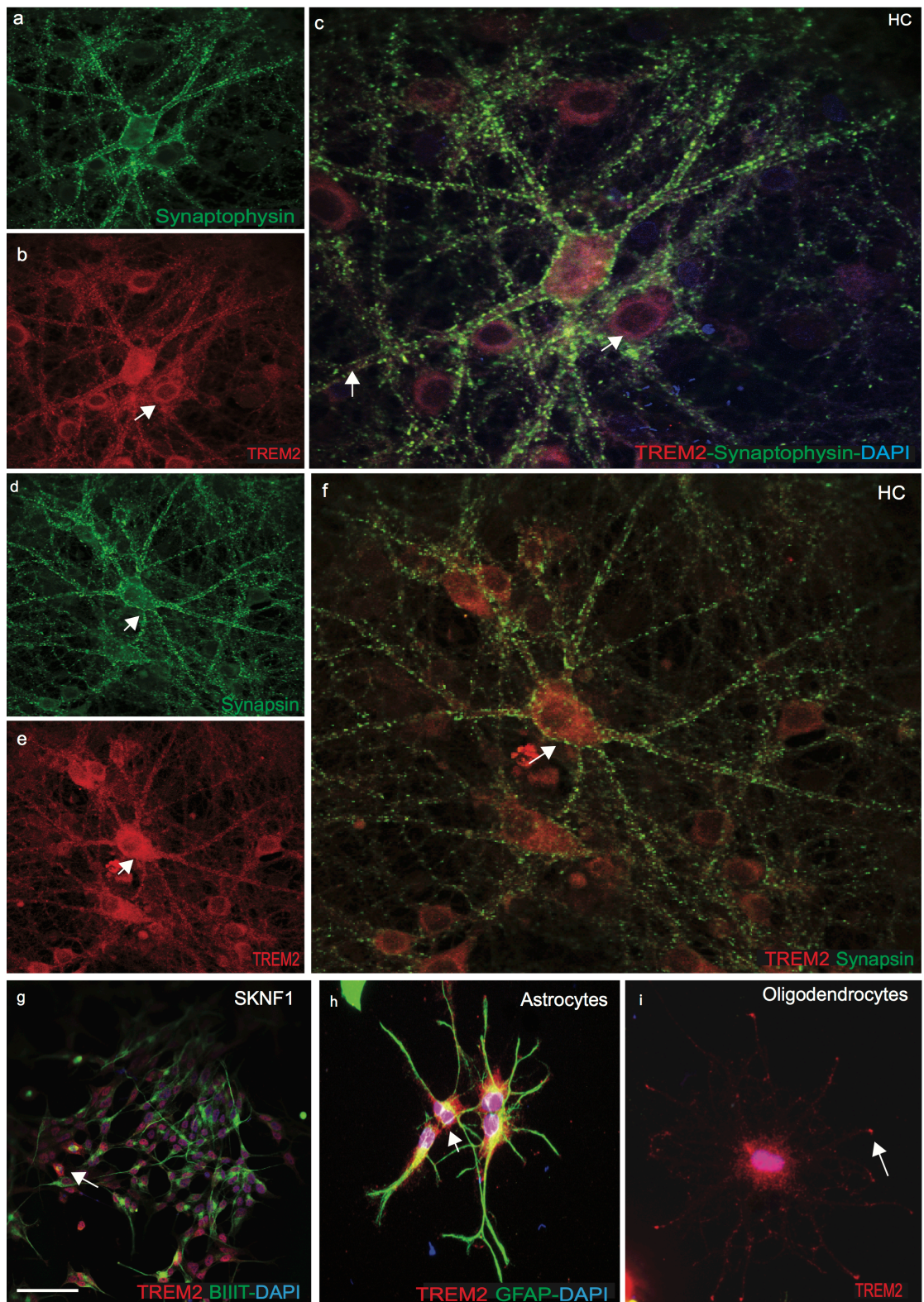


Figure 6:

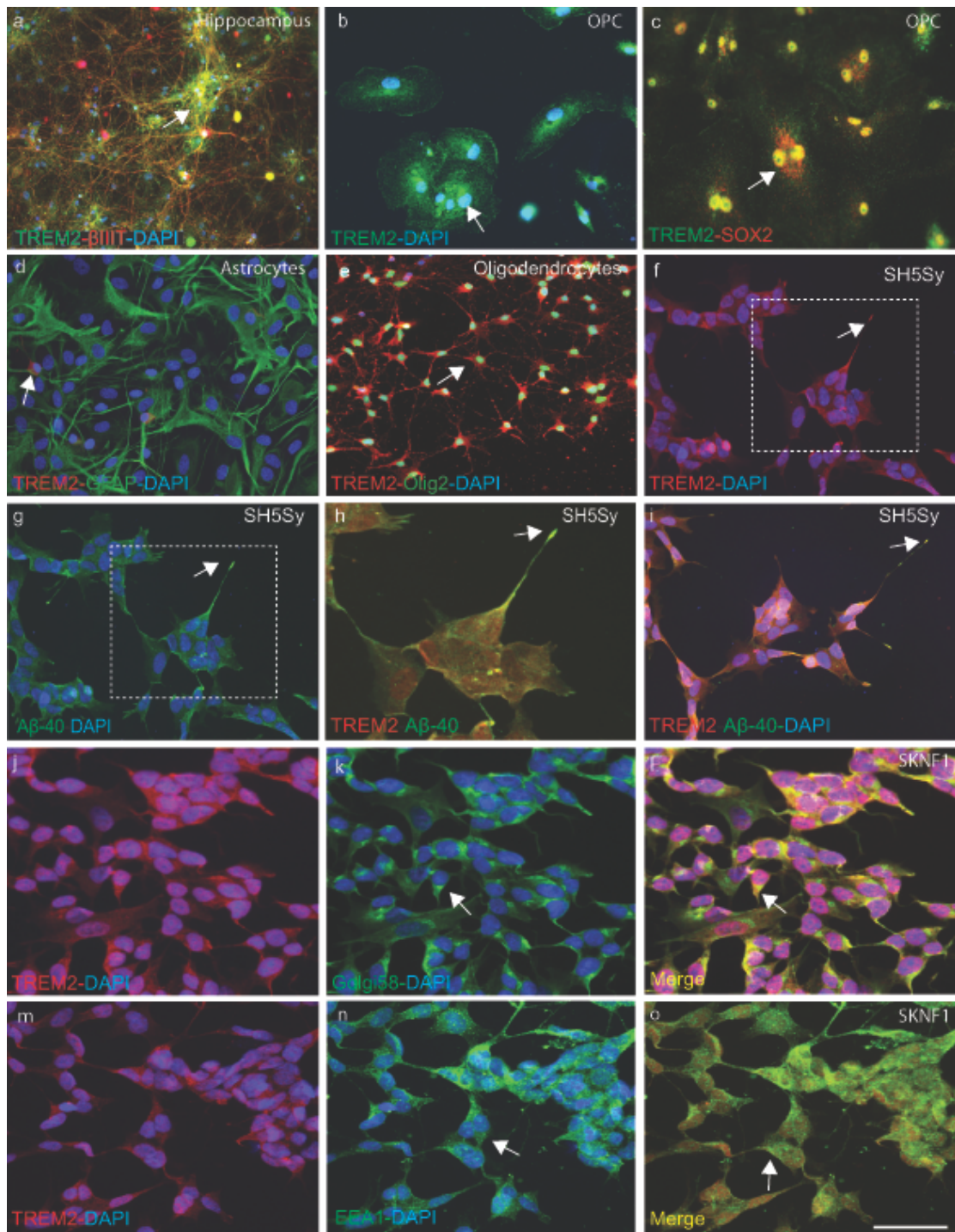


Figure 7:

